

Structural Basis for a Quadratic Relationship between Electronic Absorption and Electronic Paramagnetic Resonance Parameters of Type 1 Copper Proteins

*Sheng-Song Yu,^{†ad} Jun-Jie Li,^{†bd} Chang Cui,^d Shiliang Tian,^d Jie-Jie Chen,^a Han-Qing Yu,^{*a}
Changjun Hou,^{*b} Mark J. Nilges^{*c} and Yi Lu^{*d}*

^a Department of Applied Chemistry, University of Science & Technology of China, Hefei, Anhui, 230026, P.R. China

^b Key Laboratory of Biorheology Science and Technology, Ministry of Education, College of Bioengineering, Chongqing University, Chongqing 400044, P. R. China

^c School of Chemical Sciences Electron Paramagnetic Resonance Lab, University of Illinois at Urbana-Champaign, Urbana, IL 61801, United States

^d Department of Chemistry, University of Illinois at Urbana-Champaign, Urbana, IL 61801, United States

*** Corresponding authors**

Han-Qing Yu: hqyu@ustc.edu.cn

Changjun Hou: houcj@cqu.edu.cn

Mark J. Nilges: mjnilges@illinois.edu

Yi Lu: yi-lu@illinois.edu

ABSTRACT: Type 1 copper (T1Cu) proteins play important roles in electron transfer in biology, largely due to the unique structure of the T1Cu center, which is reflected by its spectroscopic properties. Previous reports have suggested a correlation between a high ratio of electronic absorbance ~ 450 nm to that of ~ 600 nm ($R = A_{450}/A_{600}$) and a large copper(II) hyperfine coupling in the z direction (A_z) in electron paramagnetic resonance (EPR). However, this correlation does not have a clear physical meaning, nor does it hold for many proteins with a perturbed T1Cu center. To address this issue, a new parameter of R' ($A_{450}/(A_{450}+A_{600})$) with a better physical meaning of a fractional S_{Cys} pseudo- σ to Cu(II) CT transition intensity is defined and a quadratic relationship between R' and A_z is found based on a comprehensive analysis of UV-vis absorption, EPR and structural parameters of T1Cu proteins. We are able to find good correlations between R' and the distance of copper displacement out of the trigonal plane defined by the His₂Cys ligands and the angle between the N_{His1}-Cu-N_{His2} plane and the S_{Cys}-Cu-axial ligand plane, providing a structural basis for the observed correlation. These findings and analyses provide a new framework for deeper understanding the spectroscopic and electronic properties of T1Cu proteins, which may allow better design and applications of this important class of protein for redox and electron transfer functions.

■ INTRODUCTION

Type 1 copper (T1Cu) proteins are a major class of redox proteins involved in many electron transfer processes in biology, from photosynthesis to respiration.¹⁻⁷ They perform the important functions due to several unique structural characteristics and associated electronic structural properties, and these properties are often reflected in their spectroscopic signatures. Among the unique structural characteristics is a short Cu(II)-thiolate bond coordinated by a conserved cysteine, resulting in strong electronic absorption bands due to ligand (thiolate) to metal charge transfer (CT) transitions in the visible regions, specifically S_{Cys} pseudo- σ to Cu(II) CT transition ~ 450 nm, and S_{Cys} π to Cu(II) CT transition ~ 600 nm.⁸⁻¹⁴ Depending on slight geometric differences in the T1Cu site, the intensity of electronic absorption bands from these CT transitions can vary. Spectroscopic and computational studies have indicated a strong correlation between the T1Cu structures and ratio of electronic absorbance of the ~ 450 nm band to that of the ~ 600 nm band ($R = A_{450}/A_{600}$), as a trigonal T1Cu center that is characteristic to a classic blue T1Cu center such as in azurin give rises to a spectrum with a very low R due to the dominant S_{Cys} π to Cu(II) CT transition at ~ 600 nm.¹⁵⁻¹⁸ On the other hand, a high R can be derived from either tetragonal or tetragonal distortion from the above classic T1Cu center, as observed in stellacyanin and nitrite reductases.¹⁵ Instead of extreme high or low R , most T1Cu proteins display a range of R 's.

In addition to resulting in strong electronic absorption bands, the high covalency of the Cu(II)-thiolate bond gives rise to a characteristic EPR spectrum for which the copper hyperfine splitting along the z direction (A_z or A_{\parallel}) is smaller ($< 93.5 \times 10^{-4} \text{ cm}^{-1}$) than that observed for typical copper complexes or similar sites in proteins, usually called Type 2 copper centers. Previous reports have suggested a correlation between a high R and a large A_z .^{3-5, 19-23} However, the correlation does not have a clear physical meaning, nor does it hold for many proteins with a perturbed T1Cu center

that can result from tetragonal or tetragonal distortion from the classic T1Cu center. For example, as shown in **Figure 1** and **Table 1**, even though both cucumber basic protein and nitrite reductase show values of A_z ($\sim 60 \times 10^{-4} \text{ cm}^{-1}$ and $68 \times 10^{-4} \text{ cm}^{-1}$, respectively), their R values are very different (0.6 and 1.3, respectively). Therefore, despite decades of spectroscopic and electronic structural studies of the T1Cu proteins, this interesting and intriguing correlation between electronic absorption and EPR properties remains to be understood, especially the structural basis for the correlation. To address this issue, we report herein a comprehensive analysis of UV-Vis and EPR parameters of a number of T1Cu proteins and their variants reported in the literature and produced in our lab.²⁴⁻³⁰ Most of these data have been previously published, while some are reported here for the first time. In addition, for some of previously published data, Gaussian fits of the UV-vis absorption bands and simulations of EPR data were carried out in order to improve accuracy of the absorption bands and hyperfine and g parameters in the x and y directions. These more comprehensive data analyses reveal an interesting quadratic relationship between A_z of EPR and R' ($A_{450}/(A_{450}+A_{600})$), which has a better physical meaning of a fractional S_{Cys} pseudo- σ to Cu^{II} CT transition intensity. A careful examination of structural parameters of T1Cu center has also revealed good correlation between R' and distance of copper displacement out of the trigonal plane defined by the His₂Cys ligands and the angle between the N_{His1}-Cu-N_{His2} plane and the S_{Cys}-Cu-axial ligand plane, providing a structural basis for the correlation.

■ EXPERIMENTAL SECTION

Protein Purification and Spectroscopy Collection. The M121H/H46E/F114N-, M121L-, M121E-, M121Q- and M121G-azurins were constructed, expressed and purified to homogeneity using a protocol reported previously.²⁴ Aliquots of metal-free azurin mutants in ammonia acetate

buffer (50 mM, pH 6.35) were titrated with 2 eq. Cu²⁺ and stirred at room temperature for 30 minutes. Excess copper ion was removed using a PD-10 desalting column containing 8.3 ml of SephadexTM G-25 medium. Before measurement, the buffer was exchanged to 25 mM MOPS (3-(N-morpholino) propanesulfonic acid) at pH 7.0 with Amicon® Ultra-4 centrifugal filter devices with a 10 kDa molecular weight cutoff. Small laccase from *Streptomyces coelicolor* was purified based on a procedure in the literature.³¹ The UV-vis spectra of these proteins were collected using an Agilent 8453 photodiode array spectrometer under room temperature. The X-band EPR data were collected using an X-band Varian E-122 spectrometer equipped with an Air Products Helitran cryostat and temperature controller at the Illinois EPR Research Center. The protein concentration was 1.5 mM in MOPS containing 20% glycerol. There is evidence based upon high-frequency EPR studies³² and our simulation of X-band spectra, that T1Cu center can exist in more than one state, typically in two states, with differences in rhombicity and with corresponding differences in R' values. This two-state model is supported by a theoretical study of the copper-cysteine bond in T1Cu proteins.³³ For the systems studied here, such as M121G azurin, simulation of X-band EPR spectra indicated that the differences in rhombicity are small. Besides, no resolution of the UV-Vis spectra into multiple species is achievable. As a result, for such inhomogeneous systems, the measured EPR rhombicities and UV-Vis R values will represent a weighted average.

■ RESULTS AND DISCUSSION

Poor correlation between R and A_z . The parameter R has been used in the literature for T1Cu proteins to represent the ratio of absorbance of the ~450 nm to the ~600 nm peaks, and a correlation between R and A_z of EPR has been proposed.^{3-5, 20-23} We have collected the values of R from UV-Vis data as well as g and A values from EPR results for a number of T1Cu proteins

reported in literature and listed them in **Table 1**. Since there are many reports on T1Cu proteins that expand for >50 years, we choose these proteins because we can find UV-vis and EPR spectra with well-defined absorption bands in the 450 and 600 nm region (**Figure S1**), as well as EPR data with simulation and determination of A_x , A_y and A_z . In addition, since we are seeking structural basis for this correlation, we choose proteins that have crystal structures. To obtain more accurate data and to fill in gaps in the plots shown below, we have prepared and collected UV-vis and EPR data for some T1Cu proteins, namely small laccase (SLAC) from *Streptomyces coelicolor* and M121L-, M121Q- and M121G-azurin (**Figure S2**). When we plot the R vs. A_z and $A_x - A_y$ using the data in **Table 1**, we see from **Figure 1a** that A_z and $A_x - A_y$ have a poor correlation with R, as many data points are outside the 95% confidence range and the coefficient of determination (R^2) is also low.

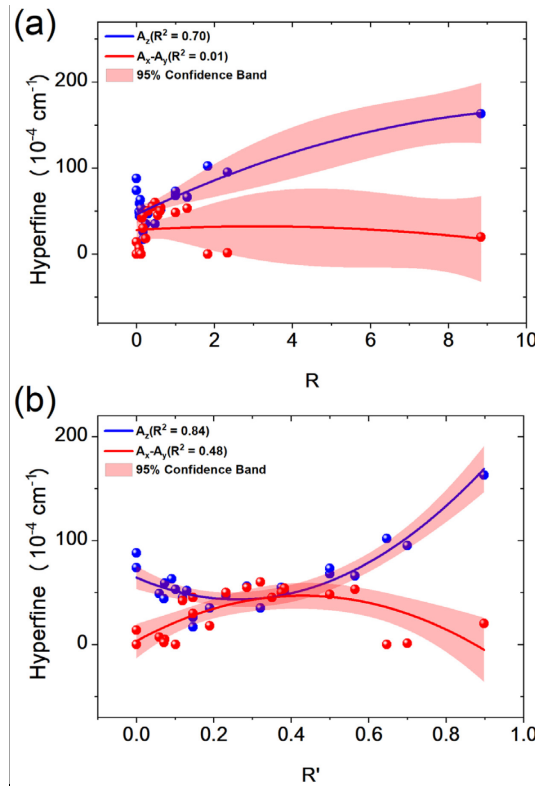


Figure 1. Correlation between R (a) and R' (b) vs A_z and $A_x - A_y$.

Table 1. EPR parameters of different type 1 copper proteins.

Protein System	Organism	R= A ₄₅₀ /A ₆₀₀	R'= A ₄₅₀ /(A ₄₅₀ + A ₆₀₀)	A _z 10 ⁻⁴ cm ⁻¹	A _x -A _y 10 ⁻⁴ cm ⁻¹	g _z	g _x	g _y	A _x 10 ⁻⁴ cm ⁻¹	A _y 10 ⁻⁴ cm ⁻¹
Laccase, fungal ³⁴	<i>Polyporus versicolor</i>	~0	0	88	0	2.190	2.042	2.042	9	9
Laccase, small ^a	<i>Streptomyces coelicolor</i>	~0	0	74	14	2.215	2.031	2.033	19	5
Azurin ^[21]	<i>P. aeruginosa</i>	0.079	0.073	59	5	2.264	2.039	2.056	9	4
M121L Azurin ^a	<i>P. aeruginosa</i>	0.062	0.059	49	7	2.268	2.038	2.051	13	20
M121L/N47S/F114N Azurin ^a	<i>P. aeruginosa</i>	0.076	0.071	44	2	2.289	2.033	2.055	19	21
Plastocyanin ^{23, 35}	<i>Spinach chloroplasts</i>	0.100	0.091	63	/	2.226	2.042	2.059	<17	<17
Amicyanin ³⁶	<i>Paracoccus denitrificans</i>	0.113	0.101	56	/	2.240	2.060	2.006	/	/
M121Q/F114P Azurin ²⁴	<i>P. aeruginosa</i>	0.135	0.119	45	42	2.250	2.036	2.041	43	1
Lipocyanin ³⁷	<i>Streptomyces coelicolor</i>	0.150	~0.130	52	/	2.273	2.038	2.053	/	/
M121Q Azurin ^a	<i>P. aeruginosa</i>	0.171	0.146	26	45	2.279	2.018	2.079	72	27
M121G Azurin ^{38,a}	<i>P. aeruginosa</i>	0.171	0.146	17	30	2.299	2.022	2.079	61	31
Stellacyanin ³⁹	<i>Rhus vernicifera</i>	0.235	0.190	35	28	2.287	2.025	2.077	57	29
Auracyanin ⁴⁰	<i>Chloroflexus aurantiacus</i>	0.300	0.232	47	50	2.210	2.018	2.062	62	12
Rusticyanin ⁴¹	<i>Acidithiobacillus ferrooxidans</i>	0.400	0.286	56	55	2.217	2.020	2.062	64	9
PseudoAzurin ⁴²	<i>Sinorhizobium meliloti</i>	0.473	0.321	35	60	2.221	2.019	2.060	69	9
Rusticyanin ⁴³	<i>Thiobacillus ferro-oxidans</i>	0.540	0.351	45	45	2.229	2.019	2.064	65	20
Cucumber basic protein ^{35, 44}	<i>Cucumber peel</i>	0.600	0.375	55	50	2.207	2.020	2.070	60	~10
PseudoAzurin ³⁵	<i>Paracoccus pantotrophus</i>	0.620	0.383	52	54	2.200	2.014	2.065	65	11
Nitrite Reductase ⁴⁵	<i>Rhodobacter sphaeroides</i>	1.000	0.500	68	48	2.190	2.020	2.060	48	0
Nitrite Reductase ^{23, 35}	<i>Achromobacter cycloclastes</i>	1.000	0.500	73	/	2.190	2.020	2.060	/	/
AcoP ⁴¹	<i>Acidithiobacillus ferrooxidans</i>	1.300	0.565	66	53	2.193	2.019	2.057	65	12
M121H Azurin ⁴⁶	<i>Alcaligenes nitrificans</i>	1.830	0.647	102	0	2.247	2.046	2.046	9	9
M121E Azurin ^a	<i>P. aeruginosa</i>	2.338	0.700	95	1	2.292	2.053	2.061	7	8
M121H/H46E/F114P Azurin ⁴⁷	<i>P. aeruginosa</i>	8.730	0.897	163	20	2.237	2.037	2.038	29	9

^a data collected from this work.

Definition of a new parameter R' for electronic absorption bands from CT transition and correlation between R' and copper hyperfine coupling. To overcome the limitation of R , we propose in this work to define a new parameter, $R' = A_{450}/(A_{450}+A_{600})$, which represents approximately the fraction of S_{Cys} pseudo- σ -Cu bond character. Likewise, $1 - R'$ represents the fraction of S_{Cys} pseudo- π -Cu bond character and both R' and $1 - R'$ range from 0 to 1. When we plotted A_z versus R' as shown in Figure 1b, we found a U-shaped dependence on R' , which is most easily fitted with a quadratic equation. In comparison with the correlation with R , most data fit into the 95% confidence band, with much improved R^2 . This dependence indicates that a larger parallel hyperfine splitting is expected when R' is small or when it approaches one. In addition, a quadratic relationship is also found between A_x-A_y and R' (Figure 1b), although the correlation, specifically, the confidence windows, is better for A_z than for A_x-A_y . We attribute the better fit using R' to defining the S_{Cys} pseudo- σ -Cu(II) bond character (R') and S_{Cys} π to Cu(II) bond character ($1 - R'$) separately, instead of the ratio of the two bonding characters (R). As a result, R is as clustered together as R' for small values of R , but as the σ character approaches 100%, the correlation using R breaks down, while that using R' still works.

The correlation between R' and A_x-A_y (and to a lesser extent for A_z) can be attributed to changing of the percent copper character in the ground state wavefunction and mixing d_{z2} into d_{x2-y2} ground state orbital character:

$$\Psi = a|d_{x2-y2} > - b|d_{z2} > \quad \text{Eq. 1}$$

a and b are the d_{x2-y2} and d_{z2} contributions to the ground state wavefunction, respectively. (Note: the ground state orbital can be written including contributions from the three other 3d orbitals, but contributions from these orbitals are equivalent to a rotation of axes.) This admixture is expected

to give rise to rhombicity to both g and to the copper hyperfine. For the rhombicity in the copper hyperfine coupling, the expected difference, can be approximated as:^{48, 49}

$$A_x - A_y = P_d [\alpha^2 8/7\sqrt{3}ab + (g_x - g_y)] \quad \text{Eq. 2}$$

Where P_d is $\sim 396 \times 10^{-4} \text{ cm}^{-1}$ and α^2 represents the spin density localized on the copper, which is expected to be on the order of 0.4 to 0.7.^{15, 23, 50} When $g_x - g_y$ is small, $A_x - A_y$ will be proportional to α^2 and b . From **Table 1**, the magnitude of $A_x - A_y$ can be as great as 40 to $60 \times 10^{-4} \text{ cm}^{-1}$, indicating that the amount of d_z^2 mixing is on the order of a few percent. The rhombicity in A is greatest for $R' \sim 0.5$, which is where the π/σ character is roughly 50/50, indicating a combined effect of copper covalency and d_{z2} mixing. For systems with either large π or large σ character, the rhombicity in A is small. For such systems $A_x - A_y$ is small and the copper hyperfine along the x and y directions is fairly small and not well resolved. Many studies in the past assumed that the g and A couplings are axial and assumed $A_x - A_y$ is zero. In Table 1, for a number of reported systems A_x and A_y were not even reported. Even in the case of systems with marked hyperfine rhombicity, such as cucumber basic protein, the hyperfine along the y direction was assumed to be zero. Thus, the accurate measurement of $A_x - A_y$ is problematic for many systems reported in the literature when this issue was not considered in the studies.

A better fit between R' and EPR parameters is observed for the value of A_z , even though A_z is expected to give a smaller change with b :^{48, 49}

$$A_z = -P_d [\kappa + 4/7\alpha^2(a^2 - b^2) - \Delta g_z - 3/14(\Delta g_x + \Delta g_y)] \quad \text{Eq. 3}$$

Where κ is the isotropic Fermi contact term, Δg_x , Δg_y and Δg_z indicate the differences between g values and 2.0023, A_z depends on $(a^2 - b^2)$, indicating that the A_z is relatively insensitive to changes in b when b is small. A decrease in A_z can be attributed in part to an increase in the Δg_z term, which results from a decrease in the energy splitting of the $d_{x^2-y^2}$ and the d_{xy} orbitals. This change has

been attributed to changes in the interaction with the axial ligand.¹⁵ A_z is also dependent on the Fermi contact term as well as the so-called spin-other-orbit terms (last term, approximated by assuming $a \gg b$). Because these terms can often add out of phase (subtract) from the other aforementioned terms, they can have a much more noticeable effect on A_z than expected. As seen from **Figure 1b**, the magnitude of A_z is larger for a system with predominately σ character as opposed to a system with predominately π character. This has been attributed to the highly covalent Cu-S(Cys) π interaction that significantly lowers the percent copper character in the ground state wavefunction.⁵¹

Correlation between R' and g values. Changing in covalency and mixing of $d_{x^2-y^2}$ and d_{z^2} ground state orbitals are also expected to affect the rhombicity of g and the value of g_z . Therefore, we also examined whether there is a correlation with R' and g values. Based on the data presented in **Table 1**, we plotted Δg_z and g_x-g_y against either R or R' (see **Figure S3** and found minimal correlation for Δg_z and g_x-g_y . The rhombicity in g due to admixture of d orbitals can be approximated with crystal field theory:^{48, 52}

$$g_x - g_y = \alpha^2 8\sqrt{3}Kab \quad \text{Eq. 4}$$

Where K is the ratio of spin-orbit coupling to the excitation energy. In the case of T1Cu centers, the g rhombicity is also expected to depend upon terms due to the interaction of the spin density delocalized on the S atom of the cysteine ligand as a result of the sulfur spin-orbit coupling (382 cm⁻¹).⁵³ In the case of the hyperfine, the rhombicity should be independent of the effects of spin density on the sulfur atom and the correlation to R' is better than that observed for the g rhombicity. Thus, for this system, the rhombicity in g is not a good parameter to quantify the admixture of the d_{z^2} orbital and does not correlate well with R' .

A caveat for these analyses is that we have used UV-vis absorption bands collected mostly at room temperature, while using the EPR parameters collected at lower temperature ($\sim 77\text{K}$), because most spectroscopic UV-vis and EPR data are reported this way in the literature. This difference in temperature may have contributed to less-than-ideal correlation we have found, but the finding is still useful for most researchers in the field who continue to collect the data at different temperatures.

Structural basis for correlation between R' and A values. Our analyses of the UV-vis and EPR data have allowed us to find that correlation between R' and the rhombicity in A (the value of A_z) gives a rise to a quadratic dependence. The maximum in A_x-A_y and the minimum in A_z occur when R' ranges from 0.45 and 0.27, respectively. The increase in rhombicity from more typical blue T1Cu proteins has been attributed to distortion from the idealized trigonal planar geometry, with fungal laccase being the best example of this idealized structure. For fungal laccase, the nearest axial ligand (Leucine) is 3.6 Å so the axial binding is extremely weak. As a result, a $d_{x^2-y^2}$ ground-state orbital with two lobes roughly (~ 15 degrees away) points along the two copper-nitrogen bonds and the other two lobes form a strong in-plane π -bond to the p_x orbital of the sulfur of the cysteine.

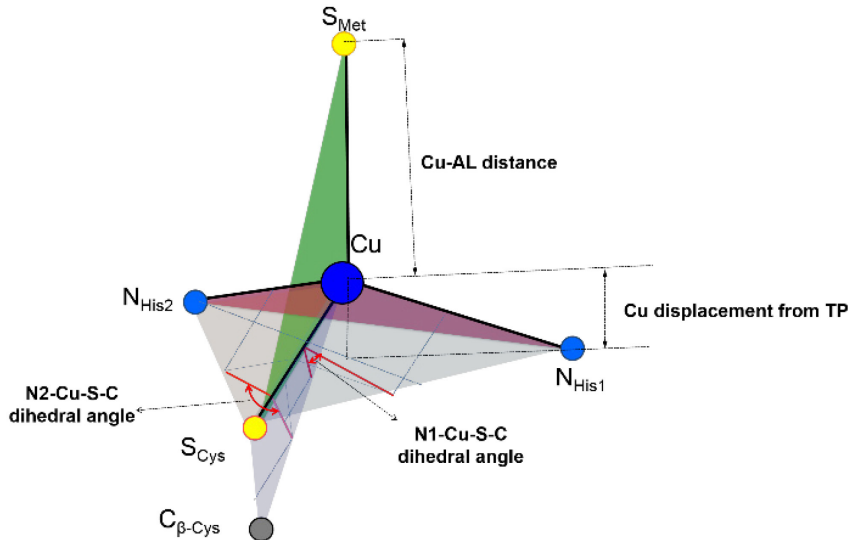


Figure 2. Illustration of geometry parameters for Cu binding site in type 1 copper proteins. AL is the axial ligand. TP is the trigonal plane defined by $N_{His1}N_{His2}S_{Cys}$. For azurin system, N_{His1} is N_{His117} and N_{His2} is N_{His46} , S_{Cys} is S_{Cys112} .

Fungal laccase, which best represents this idealized trigonal planar geometry, has a value of $90 \times 10^{-4} \text{ cm}^{-1}$ for A_z which is larger than the typical “classic” blue copper system.¹⁵⁻¹⁸ A model system for the idealized trigonal planar T1Cu system has been reported,⁵⁴ and an observed value of $111 \times 10^{-4} \text{ cm}^{-1}$ for A_z is reported. While this value is also relatively large, it is consistent with the data for fungal laccase and the data plotted in **Figure 1b**.

The increase in rhombicity and admixture of d_{z2} character is a result of distortion of this ideal trigonal plane structure in two ways. One is the interaction of an axial ligand; the stronger this interaction, the larger the displacement of the copper out of the NNS trigonal plane and the shorter the copper-axial-ligand bond, which should disrupt the $S_{Cys}\pi$ -Cu bond. A coupled distortion model has been proposed where the long axial S_{Met} -Cu bond results in a short S_{Cys} -Cu bond, opposing a Jahn-Teller tetragonal distortion of the oxidized T1Cu site.¹⁵ Therefore, when we plot the distances of copper displacement out of the trigonal plane defined by His₂Cys ligands using the data in **Table 2** vs. R' , we found a good correlation between the displacement of the copper out of the trigonal

plane and R' is (Figure 3). For the plot of distance of between the Cu and the axial ligand (Cu-AL) vs R' we found a general trend, with a few exceptions (Figure 3).

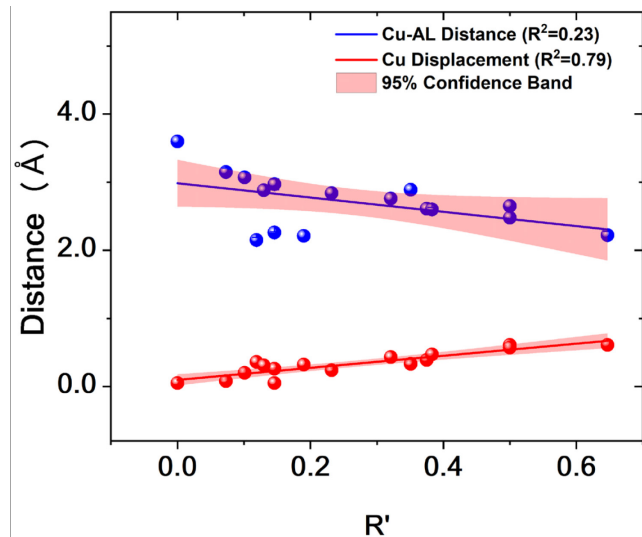


Figure 3. Correlation between the distance of copper displacement out of the trigonal plane defined by His₂Cys ligands and R' .

Table 2. Geometry of Cu binding site in type 1 copper proteins.

Protein System	Organism	Structure ID	Cu-AL distance (Å)	Cu displacement from TP (Å)	N _{His1} -Cu-S _{Cys-C_β-Cys} dihedral angle (°)	N _{His2} -Cu-S _{Cys-C_β-Cys} dihedral angle (°)	Φ (°)	NCuN/SCuAL	R'
Fungal laccase	<i>Polyporus versicolor</i>	3PXL	3.60	0.05	94.7	-91.5	82.3	0	
Azurin	<i>P. aeruginosa</i>	4AZU	3.15	0.08	98.6	-90.7	84.2		0.073
Amicyanin	<i>Paracoccus denitrificans</i>	2OV0	3.07	0.20	108.0	-95.6	81.2		0.101
M121Q/F114P Azurin	<i>P. aeruginosa</i>	3IN0	2.15	0.36	94.6	-123.9	71.9		0.119
Plastocyanin	<i>Spinach chloroplasts</i>	1AG6	2.88	0.31	110.1	-104.5	80.1		0.130
M121Q Azurin	<i>P. aeruginosa</i>	1URI	2.26	0.26	106.2	-105.1	83.8		0.146
M121G Azurin	<i>P. aeruginosa</i>	4MFH	2.97	0.05	100.1	-85.2	74.0		0.146
Stellacyanin	<i>Rhus vernicifera</i>	1JER	2.21	0.32	109.2	-107.3	83.5		0.190
Auracyanin	<i>Chloroflexus aurantiacus</i>	1QHQ	2.84	0.24	109.1	-99.2	73.2		0.232
Pseudoazurin	<i>Sinorhizobium meliloti</i>	1PAZ	2.76	0.43	117.8	-110.1	72.1		0.321
Rusticyanin	<i>Thiobacillus ferro-oxidans</i>	1RCY	2.89	0.33	104.4	-110.5	77.1		0.351
Cucumber protein	basic	<i>Cucumber peel</i>	2CBP	2.61	0.39	118.4	-109.3	69.6	0.375
Pseudoazurin		<i>Paracoccus pantotrophus</i>	3ERX	2.60	0.47	118.7	-113.6	74.1	0.383
Nitrite Reductase		<i>Achromobacter cycloclastes</i>	1NIC	2.65	0.57	116.6	-125.9	61.4	0.500
Nitrite Reductase		<i>Rhodobacter sphaeroides</i>	1ZV2	2.48	0.61	118.6	-129.0	62.5	0.500
M121H Azurin		<i>Achromobacter nitrificans</i>	1A4A	2.22	0.61	121.5	-122.5	65.2	0.647

Intertwined with the change in axial ligand binding is the increase in pseudo-tetrahedral character due to the resultant flattening of the resultant trigonal pyramidal structure.²³ **Table 2** shows the angle Φ , which is the angle between the $\text{N}_{\text{His}1}\text{-Cu-N}_{\text{His}2}$ plane and the $\text{S}_{\text{Cys}}\text{-Cu-AL}$ plane. For systems with R' close to 0, the interplane angle, Φ , which is expected to result in a strong Cu-S pi-bond is close to 90°. As R' increases, the interplane angle, Φ , roughly moves towards 60°. Although there is a general trend, there is a fair amount of scatter, particularly in the region for R' equal to 0.1 to 0.2.

The strength of the in-plane S_{Cys} π -Cu bond will depend upon the $\text{N}_{\text{His}}\text{-Cu-S}_{\text{Cys}}\text{-C}_{\beta}\text{-Cys}$ dihedral angles. As shown in **Figure 4**, which is based on data in **Table 2**, for T1Cu proteins with $R' \sim 0$, these angles are close to 90° as expected, while for Type 1.5 Cu systems with R' close to 1, these angles are close to 120°. For intermediate values of R' , these angles vary between 90° and 120° with a rough correlation to R' . There are some points that do not fit that well on the curve, such as M121Q/F114P Azurin, which has markedly different $\text{N}_{\text{His}}\text{-Cu-S}_{\text{Cys}}\text{-C}_{\beta}\text{-Cys}$ dihedral angles.

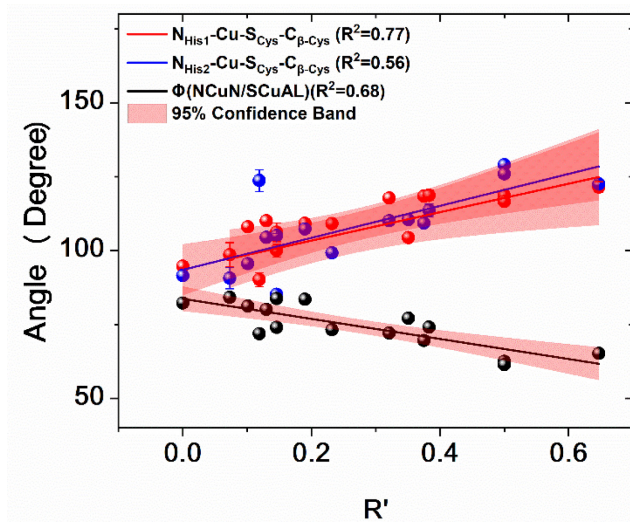


Figure 4. Correlation between R' and $\text{N}_{\text{His}}\text{-Cu-S}_{\text{Cys}}\text{-C}_{\beta}\text{-Cys}$ dihedral angles or the angle Φ between the $\text{N}_{\text{His}1}\text{-Cu-N}_{\text{His}2}$ plane and the $\text{S}_{\text{Cys}}\text{-Cu-AL}$ plane.

We find no one structural parameter correlates tightly with R' , which implies that changes in geometry in the series are more complex and involve more than a simple singular change in geometry. Added to this is the fact the axial ligand varies in the series examined, and differences in binding between O, N, and S probably play a role.

Just as fungal laccase is representative of the blue, strong π Cu-S_{Cys} end of the spectrum ($R' \sim 0$), M121H and M121H/H46E/F114P azurin are representative of the green strong σ Cu-S_{Cys} end of the spectrum (R' close to 1). It is interesting to note that for both ends, the rhombicity of ground state orbital (as measured by g and A) is close to zero. The geometric structure of M121H is close to a (C_{2v}) distorted pseudo-tetrahedral⁵⁵ (see figure 2 in reference 55; note: the y and z directions are interchanged between those defined in reference 47) with a d_{xy} ground state orbital primarily aligned with the N_{His1}-Cu-N_{His2} plane with the lobes of the orbital roughly coincident with the N_{His}-Cu bonds. The S_{Cys}-Cu-AL plane is rotated out from the d_{yz} plane by as much as 30°, which allows some mixture of the d_{yz} orbital into the ground state, but this mixture primarily causes a tilting of the d_{xy} orbital rather than adding rhombic character (d_z² mixing) to the ground state orbital.^[47] This rotation of the S_{Cys}-Cu-AL plane is driven by the Jahn-Teller stabilization which results in lifting the degeneracy of the d_{yz} and d_{xy} orbitals expected for a tetrahedral geometry.

Spectroscopic and computational studies by Solomon and other groups have classified the T1Cu centers into classic and perturbed T1Cu, with spectroscopic features arising from different degrees S_{Cys} pseudo- σ to Cu(II) CT transition ~450 nm, and S_{Cys} to Cu(II) CT transition ~600 nm. The classic T1Cu (e.g., azurin) would correspond to $R' < 0.15$, while the perturbed T1Cu would display $R' > 0.15$. In our model described in this work, we consider a spectrum of systems ranging from pure S_{Cys} π to Cu(II) CT transition to pure S_{Cys} pseudo- σ to Cu(II) CT transition and as such, azurin would be considered perturbed but only by a small amount. The previous studies did not clarify

how the perturbed model would apply to systems that are mainly S_{Cys} pseudo- σ to Cu(II) CT transition (i.e., $R' = 1$), which can be described as being due to either a highly perturbed T1Cu or plain Type 2 Cu. By identifying the quadratic correlation, this work avoids this artificial division and just consider R' ranging from 0 to 1, pure π to pure σ , blue to green. More importantly, by finding the structural basis for the correlation (see Figures 3 and 4), we have identified the perturbation through not only the NCuN/SCuAL angle, but also the character of S_{Cys} -Cu-AL bond, which is intertwined.

■ CONCLUSION

In conclusion, we have examined the correlation of UV-vis absorption, EPR, and structural parameters for a number of T1Cu proteins. We find the best correlation between A_z of the copper hyperfine coupling with a newly defined R' ($A_{450}/(A_{450}+A_{600})$). To a smaller extent we observed a correlation between the rhombicity of copper hyperfine coupling (A_x-A_y) and R' . The correlation between R' and A_z and A_x-A_y are quadratic in form so that at values of R' either very close to 0 or near 1 one can expect to see similar near axial EPR spectra with A_z values in the range around $100 \times 10^{-4} \text{ cm}^{-1}$. We have explained the correlations by the structural parameters, including the distance of copper displacement out of the trigonal plane defined by His₂Cys ligands and the angle between the N_{His1}-Cu-N_{His2} plane and the S_{Cys} -Cu-axial ligand plane and corresponding molecular orbitals of the T1Cu centers.

The correlation reported in this work is primarily an empirical observation and the simplest fit to a U-shaped curve is a quadratic relationship. Despite the empirical observation, the correlation can be explained in terms of changing in covalency and mixing d_{z2} character in the ground state orbital and geometry. A_x-A_y is a direct measure of the d_{z2} character and shows a curve with a

maximum at $R' \sim 0.5$. This is the point where system is roughly 50/50 π/σ and represents an intermediate geometry between trigonal planar and pseudo-tetrahedral. For $R' = 0$ or 1 the geometry is fairly well defined, and the ground state is $d_{x^2-y^2}$ or d_{xy} with no d_{z^2} mixing. Now A_x - A_y is difficult to accurately measure, so we have looked instead to see if A_z , which is easy to measure correlates with R' . While A_x - A_y is a direct measure of d_{z^2} mixing, A_z is not, but it is still dependent upon the d_{z^2} character as discussed in this work. Unlike A_x - A_y , the A_z curve has a minimum at $\sim R' = 0.3$ not at $\sim R' = 0.5$ which is where the d_{z^2} mixing should be greatest. This is in part be due to the fact that A_z for a pure π T1Cu system is about half that a pure σ type 1.5 Cu system. These findings and analyses provide a new framework for deeper understanding the spectroscopic and electronic properties of T1Cu proteins, which may allow better design and applications of this important class of protein for redox and electron transfer functions.

■ ASSOCIATED CONTENT

Supporting Information

The Supporting Information is available free of charge at <https://pubs.acs.org/xxxxxx>.

UV-vis absorption of T1Cu proteins, EPR of some azurin mutations and SLAC, correlation between R and R' vs. Δg_z and g_x-g_y .

■ AUTHOR INFORMATION

Corresponding Authors

Han-Qing Yu - Department of Applied Chemistry, University of Science & Technology of China, Hefei, Anhui, 230026, P. R. China;
Email: hqyu@ustc.edu.cn

Changjun Hou - Key Laboratory of Biorheology Science and Technology, Ministry of Education, College of Bioengineering, Chongqing University, Chongqing 400044, P. R. China;
Email: houcj@cqu.edu.cn

Mark J. Nilges - School of Chemical Sciences Electron Paramagnetic Resonance Lab, University of Illinois at Urbana-Champaign, Urbana, IL 61801, United States;
Email: mjniilges@illinois.edu

Yi Lu - Department of Chemistry, University of Illinois at Urbana-Champaign, Urbana, IL 61801, United States;
Email: yi-lu@illinois.edu

Authors

Sheng-Song Yu - Department of Applied Chemistry, University of Science & Technology of China, Hefei, Anhui, 230026, P.R. China;

Jun-Jie Li - Key Laboratory of Biorheology Science and Technology, Ministry of Education, College of Bioengineering, Chongqing University, Chongqing 400044, P. R. China;

Chang Cui - Department of Chemistry, University of Illinois at Urbana-Champaign, Urbana, IL 61801, United States;

Shiliang Tian - Department of Chemistry, University of Illinois at Urbana-Champaign, Urbana, IL 61801, United States;

Jie-Jie Chen - Department of Applied Chemistry, University of Science & Technology of China, Hefei, Anhui, 230026, P.R. China

Author Contributions

[†]These authors contributed equally to this work. All authors have given approval to the final version of the manuscript.

Notes

The authors declare no competing financial interest.

■ ACKNOWLEDGEMENTS

We thank US National Science Foundation (CHE-1710241) for financial support. Some EPR data was collected using an X-band EPR Spectrometer purchased with fund from the US National Science Foundation under 1726244.

■ REFERENCES

- (1) Gray, H. B.; Malmström, B. G.; Williams, R. Copper Coordination in Blue Proteins. *J. Biol. Inorg. Chem.* **2000**, *5*, 551-559.
- (2) Vila, A. J., Fernández, C. O., In *Handbook on Metalloproteins*, Bertini, I., Sigel, A., Sigel, H., Ed. Marcel Dekker: New York, 2001; pp 813-856.
- (3) Lu, Y., Electron Transfer: Cupredoxins. In *Comprehensive Coordination Chemistry II: From Biology to Nanotechnology*, Que, L., Tolman, W. B., Ed. Elsevier: Oxford, 2004; Vol. 8, pp 91-122.
- (4) Solomon, E. I.; Szilagyi, R. K.; DeBeer George, S.; Basumallick, L. Electronic Structures of Metal Sites in Proteins and Models: Contributions to Function in Blue Copper Proteins. *Chem. Rev.* **2004**, *104*, 419-458.
- (5) Canters, G.; Gilardi, G. Engineering Type 1 Copper Sites in Proteins. *FEBS Lett.* **1993**, *325*, 39-48.
- (6) Dennison, C. Investigating the Structure and Function of Cupredoxins. *Coord. Chem. Rev.* **2005**, *249*, 3025-3054.
- (7) Li, H.; Webb, S. P.; Ivanic, J.; Jensen, J. H. Determinants of the Relative Reduction Potentials of Type-1 Copper Sites in Proteins. *J. Am. Chem. Soc.* **2004**, *126*, 8010-8019.
- (8) Donaire, A.; Jiménez, B.; Fernández, C. O.; Pierattelli, R.; Niizeki, T.; Moratal, J.-M.; Hall, J. F.; Kohzuma, T.; Hasnain, S. S.; Vila, A. J. Metal–Ligand Interplay in Blue Copper Proteins Studied by ^1H NMR Spectroscopy: Cu (II)–Pseudoazurin and Cu (II)–Rusticyanin. *J. Am. Chem. Soc.* **2002**, *124*, 13698-13708.
- (9) Gupta, D. D.; Usharani, D.; Mazumdar, S. Mono-Nuclear Copper Complexes Mimicking the Intermediates for the Binuclear Copper Center of the Subunit II of Cytochrome Oxidase: A Peptide Based Approach. *Dalton Trans.* **2016**, *45*, 17624-17632.
- (10) Edington, M. D.; Diffey, W. M.; Doria, W. J.; Riter, R. E.; Beck, W. F. Radiationless Decay from the Ligand-to-Metal Charge-Transfer State in the Blue Copper Protein Plastocyanin. *Chem. Phys. Lett.* **1997**, *275*, 119-126.
- (11) Sarangi, R.; Gorelsky, S. I.; Basumallick, L.; Hwang, H. J.; Pratt, R. C.; Stack, T. D. P.; Lu, Y.; Hodgson, K. O.; Hedman, B.; Solomon, E. I. Spectroscopic and Density Functional Theory

Studies of the Blue-Copper Site in M121SeM and C112SeC Azurin: Cu-Se versus Cu-S Bonding. *J. Am. Chem. Soc.* **2008**, *130*, 3866-3877.

(12) Lancaster, K. M.; George, S. D.; Yokoyama, K.; Richards, J. H.; Gray, H. B. Type-Zero Copper Proteins. *Nat. Chem.* **2009**, *1*, 711.

(13) Cohen, M. R.; Mendelman, N.; Radoul, M.; Wilson, T. D.; Savelieff, M. G.; Zimmermann, H.; Kaminker, I.; Feintuch, A.; Lu, Y.; Goldfarb, D. Thiolate Spin Population of Type I Copper in Azurin Derived from S-33 Hyperfine Coupling. *Inorg. Chem.* **2017**, *56*, 10117-10117.

(14) Berry, S. M.; Baker, M. H.; Reardon, N. J. Reduction Potential Variations in Azurin through Secondary Coordination Sphere Phenylalanine Incorporations. *J. Inorg. Biochem.* **2010**, *104*, 1071-1078.

(15) LaCroix, L. B.; Randall, D. W.; Nersessian, A. M.; Hoitink, C. W. G.; Canters, G. W.; Valentine, J. S.; Solomon, E. I. Spectroscopic and Geometric Variations in Perturbed Blue Copper Centers: Electronic Structures of Stellacyanin and Cucumber Basic Protein. *J. Am. Chem. Soc.* **1998**, *120*, 9621-9631.

(16) Pierloot, K.; De Kerpel, J. O.; Ryde, U.; Olsson, M. H.; Roos, B. O. Relation between the Structure and Spectroscopic Properties of Blue Copper Proteins. *J. Am. Chem. Soc.* **1998**, *120*, 13156-13166.

(17) Randall, D.; Gamelin, D.; LaCroix, L.; Solomon, E. Electronic Structure Contributions to Electron Transfer in Blue Cu and Cu_A. *J. Biol. Inorg. Chem.* **2000**, *5*, 16-29.

(18) Van Gastel, M.; Canters, G.; Krupka, H.; Messerschmidt, A.; de Waal, E.; Warmerdam, G.; Groenen, E. Axial Ligation in Blue-Copper Proteins. A W-Band Electron Spin Echo Detected Electron Paramagnetic Resonance Study of the Azurin Mutant M121H. *J. Am. Chem. Soc.* **2000**, *122*, 2322-2328.

(19) Lu, Y.; Roe, J. A.; Gralla, E. B.; Valentine, J. S., Metalloprotein Ligand Redesign: Characterization of Copper-Cysteinate Proteins Derived from Yeast Copper-Zinc Superoxide Dismutase. In *Bioinorganic Chemistry of Copper*, Kenneth D. Karlin, Z. T., Ed. Chapman & Hall: New York, 1993; pp 64-77.

(20) Lu, Y.; LaCroix, L. B.; Lowery, M. D.; Solomon, E. I.; Bender, C. J.; Peisach, J.; Roe, J. A.; Gralla, E. B.; Valentine, J. S. Construction of a Blue Copper Site at the Native Zinc Site of Yeast Copper-Zinc Superoxide Dismutase. *J. Am. Chem. Soc.* **1993**, *115*, 5907-5918.

(21) Han, J.; Loehr, T. M.; Lu, Y.; Valentine, J. S.; Averill, B. A.; Sanders-Loehr, J. Resonance Raman Excitation Profiles Indicate Multiple Cys. Fwdarw. Cu Charge Transfer Transitions in Type 1 Copper Proteins. *J. Am. Chem. Soc.* **1993**, *115*, 4256-4263.

(22) Andrew, C. R.; Yeom, H.; Valentine, J. S.; Karlsson, B. G.; Bonander, N.; Vanpouderoyen, G.; Canters, G. W.; Loehr, T. M.; Sandersloehr, J. Raman Spectroscopy as an Indicator of Cu-S Bond-Length in Type-1 and Type-2 Copper Cysteinate Proteins. *J. Am. Chem. Soc.* **1994**, *116*, 11489-11498.

(23) LaCroix, L. B.; Shadle, S. E.; Wang, Y. N.; Averill, B. A.; Hedman, B.; Hodgson, K. O.; Solomon, E. I. Electronic Structure of the Perturbed Blue Copper Site in Nitrite Reductase: Spectroscopic Properties, Bonding, and Implications for the Entatic/Rack State. *J. Am. Chem. Soc.* **1996**, *118*, 7755-7768.

(24) Marshall, N. M.; Garner, D. K.; Wilson, T. D.; Gao, Y. G.; Robinson, H.; Nilges, M. J.; Lu, Y. Rationally Tuning the Reduction Potential of a Single Cupredoxin Beyond the Natural Range. *Nature* **2009**, *462*, 113-127.

(25) Hadt, R. G.; Sun, N.; Marshall, N. M.; Hodgson, K. O.; Hedman, B.; Lu, Y.; Solomon, E. I. Spectroscopic and DFT Studies of Second-Sphere Variants of the Type 1 Copper Site in Azurin: Covalent and Nonlocal Electrostatic Contributions to Reduction Potentials. *J. Am. Chem. Soc.* **2012**, *134*, 16701-16716.

(26) Farver, O.; Marshall, N. M.; Wherland, S.; Lu, Y.; Pecht, I. Designed Azurins Show Lower Reorganization Free Energies for Intraprotein Electron Transfer. *Proc. Natl. Acad. Sci. U.S.A.* **2013**, *110*, 10536-10540.

(27) Clark, K. M.; Yu, Y.; Van Der Donk, W. A.; Blackburn, N. J.; Lu, Y. Modulating the Copper-Sulfur Interaction in Type 1 Blue Copper Azurin by Replacing Cys112 with Nonproteinogenic Homocysteine. *Inorg. Chem. Frontiers* **2014**, *1*, 153-158.

(28) Hosseinzadeh, P.; Marshall, N. M.; Chacón, K. N.; Yu, Y.; Nilges, M. J.; New, S. Y.; Tashkov, S. A.; Blackburn, N. J.; Lu, Y. Design of a Single Protein That Spans the Entire 2-V Range of Physiological Redox Potentials. *Proc. Natl. Acad. Sci. U.S.A.* **2016**, *113*, 262-267.

(29) Hosseinzadeh, P.; Tian, S.; Marshall, N. M.; Hemp, J.; Mullen, T.; Nilges, M. J.; Gao, Y.-G.; Robinson, H.; Stahl, D. A.; Gennis, R. B. A Purple Cupredoxin from *Nitrosopumilus Maritimus* Containing a Mononuclear Type 1 Copper Center with an Open Binding Site. *J. Am. Chem. Soc.* **2016**, *138*, 6324-6327.

(30) Yu, Y.; Petrik, I. D.; Chacón, K. N.; Hosseinzadeh, P.; Chen, H.; Blackburn, N. J.; Lu, Y. Effect of Circular Permutation on the Structure and Function of Type 1 Blue Copper Center in Azurin. *Protein Sci.* **2017**, *26*, 218-226.

(31) Machczynski, M. C.; Vijgenboom, E.; Samyn, B.; Canters, G. W. Characterization of SLAC: A Small Laccase from *Streptomyces Coelicolor* with Unprecedented Activity. *Protein Sci.* **2004**, *13*, 2388-2397.

(32) Gast, P.; Broeren, F. G.; Sottini, S.; Aoki, R.; Takashina, A.; Yamaguchi, T.; Kohzuma, T.; Groenen, E. J. The Type 1 Copper Site of Pseudoazurin: Axial and Rhombic. *J. Inorg. Biochem.* **2014**, *137*, 57-63.

(33) Ryde, U.; Olsson, M. H. M.; Roos, B. O.; Borin, A. C. A Theoretical Study of the Copper-Cysteine Bond in Blue Copper Proteins. *Theor. Chem. Acc.* **2001**, *105*, 452-462.

(34) Malmström, B. G.; Reinhamar, B.; Vänngård, T. Two Forms of Copper (II) in Fungal Laccase. *Biochim. Biophys. Acta* **1968**, *156*, 67-76.

(35) Xie, X.; Hadt, R. G.; Pauleta, S. R.; González, P. J.; Un, S.; Moura, I.; Solomon, E. I. A Variable Temperature Spectroscopic Study on *Paracoccus Pantotrophus* Pseudoazurin: Protein Constraints on the Blue Cu Site. *J. Inorg. Biochem.* **2009**, *103*, 1307-1313.

(36) Choi, M.; Sukumar, N.; Mathews, F. S.; Liu, A.; Davidson, V. L. Proline 96 of the Copper Ligand Loop of Amicyanin Regulates Electron Transfer from Methylamine Dehydrogenase by Positioning Other Residues at the Protein-Protein Interface. *Biochem.* **2011**, *50*, 1265-1273.

(37) Worrall, J. A.; Machczynski, M. C.; Keijser, B. J.; di Rocco, G.; Ceola, S.; Ubbink, M.; Vijgenboom, E.; Canters, G. W. Spectroscopic Characterization of a High-Potential Lipid-Cupredoxin Found in *Streptomyces c oelicolor*. *J. Am. Chem. Soc.* **2006**, *128*, 14579-14589.

(38) Sieracki, N. A.; Tian, S.; Hadt, R. G.; Zhang, J.-L.; Woertink, J. S.; Nilges, M. J.; Sun, F.; Solomon, E. I.; Lu, Y. Copper-Sulfenate Complex from Oxidation of a Cavity Mutant of *Pseudomonas Aeruginosa* Azurin. *Proc. Natl. Acad. Sci. U.S.A.* **2014**, *111*, 924-929.

(39) Peisach, J.; Levine, W. G.; Blumberg, W. Structural Properties of Stellacyanin, a Copper Mucoprotein from *Rhus Vernicifera*, the Japanese Lac Tree. *J. Biol. Chem.* **1967**, *242*, 2847-2858.

(40) Trost, J. T.; Mcmanus, J. D.; Freeman, J. C.; Ramakrishna, B. L.; Blankenship, R. E. Auracyanin, a Blue Copper Protein from the Green Photosynthetic Bacterium *Chloroflexus Aurantiacus*. *Biochemistry* **1988**, *27*, 7858-7863.

(41) Roger, M.; Biaso, F.; Castelle, C. J.; Bauzan, M.; Chaspoul, F.; Lojou, E.; Sciara, G.; Caffarri, S.; Giudici-Orticoni, M.-T.; Ilbert, M. Spectroscopic Characterization of a Green Copper Site in a Single-Domain Cupredoxin. *PLoS One* **2014**, *9*.

(42) Ferroni, F. M.; Marangon, J.; Neuman, N. I.; Cristaldi, J. C.; Brambilla, S. M.; Guerrero, S. A.; Rivas, M. G.; Rizzi, A. C.; Brondino, C. D. Pseudoazurin from *Sinorhizobium Meliloti* as an Electron Donor to Copper-Containing Nitrite Reductase: Influence of the Redox Partner on the Reduction Potentials of the Enzyme Copper Centers. *J. Biol. Inorg. Chem.* **2014**, *19*, 913-921.

(43) Cox, J. C.; Malmström, B. G. EPR Studies on the Blue Copper Protein, Rusticyanin. *FEBS Lett.* **1978**, *93*, 157-160.

(44) Sakurai, T.; Okamoto, H.; Kawahara, K.; Nakahara, A. Some Properties of a Blue Copper Protein 'Plantacyanin' from Cucumber Peel. *FEBS Lett.* **1982**, *147*, 220-224.

(45) Olesen, K.; Veselov, A.; Zhao, Y.; Wang, Y.; Danner, B.; Scholes, C. P.; Shapleigh, J. P. Spectroscopic, Kinetic, and Electrochemical Characterization of Heterologously Expressed Wild-Type and Mutant Forms of Copper-Containing Nitrite Reductase from *Rhodobacter Sphaeroides* 2.4.3. *J. Biochem.* **1998**, *37*, 6086-6094.

(46) Kroes, S. J.; Hoitink, C. W.; Andrew, C. R.; Ai, J.; Sanders - Loehr, J.; Messerschmidt, A.; Hagen, W. R.; Canters, G. W. The Mutation Met121→His Creates a Type-1.5 Copper Site in *Alcaligenes Denitrificans* Azurin. *Eur. J. Biochem.* **1996**, *240*, 342-351.

(47) Tian, S. L.; Liu, J.; Cowley, R. E.; Hosseinzadeh, P.; Marshall, N. M.; Yu, Y.; Robinson, H.; Nilges, M. J.; Blackburn, N. J.; Solomon, E. I.; Lu, Y. Reversible S-Nitrosylation in an Engineered Azurin. *Nat. Chem.* **2016**, *8*, 670-677.

(48) McGarvey, B. R. Electron Spin Resonance of Transition-Metal Complexes, In: Transition Metal Chemistry. *Inorg Chem* **1966**, *57*, 8078-8088.

(49) Quintanar, L.; Yoon, J. J.; Aznar, C. P.; Palmer, A. E.; Andersson, K. K.; Britt, R. D.; Solomon, E. I. Spectroscopic and Electronic Structure Studies of the Trinuclear Cu Cluster Active Site of the Multicopper Oxidase Laccase: Nature of its Coordination Unsaturation. *J. Am. Chem. Soc.* **2005**, *127*, 13832-13845.

(50) Penfield, K. W.; Gewirth, A. A.; Solomon, E. I. Electronic Structure and Bonding of the Blue Copper Site in Plastocyanin. *J. Am. Chem. Soc.* **1985**, *107*, 4519-4529.

(51) Solomon, E. I. Spectroscopic Methods in Bioinorganic Chemistry: Blue to Green to Red Copper Sites. *Inorg. Chem.* **2006**, *45*, 8012-8025.

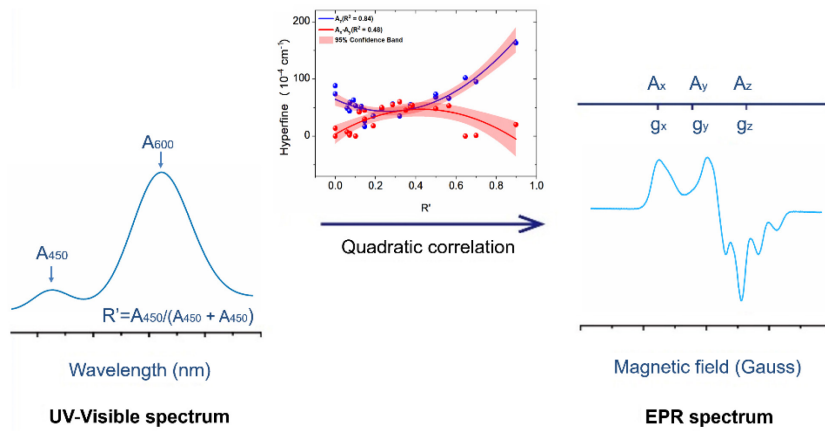
(52) Hitchman, M. The Interpretation of Rhombic G Tensors in Copper Complexes. *J. Chem. Soc. A* **1970**, 4-9.

(53) Ralle, M.; Berry, S. M.; Nilges, M. J.; Gieselman, M. D.; van der Donk, W. A.; Lu, Y.; Blackburn, N. J. The Selenocysteine-Substituted Blue Copper Center: Spectroscopic Investigations of Cys112SeCys *Pseudomonas Aeruginosa* Azurin. *J. Am. Chem. Soc.* **2004**, *126*, 7244-7256.

(54) Holland, P. L.; Tolman, W. B. Three-Coordinate Cu (II) Complexes: Structural Models of Trigonal-Planar Type 1 Copper Protein Active Sites. *J. Am. Chem. Soc.* **1999**, *121*, 7270-7271.

(55) Hoffmann, S. K.; Goslar, J. Crystal Field Theory and Epr Parameters in D₂d and C₂v Distorted Tetrahedral Copper (II) Complexes. *J. Solid State Chem.* **1982**, *44*, 343-353.

Table of contents and Synopsis:



R' ($A_{450}/(A_{450}+A_{600})$), derived from absorption intensity of charge transfer bands at 450 nm and 600 nm that represents the fraction of S_{Cys} pseudo- σ -Cu bond character in type 1 copper protein, exhibits a better quadratic relationship with hyperfine coupling in the z direction (A_z) in electron paramagnetic resonance than R (A_{450}/A_{600}) vs. A_z . Structural basis for this relationship has also been found.